Article

Palladium-Catalyzed Dual Ligand-Enabled Alkylation of Silyl Enol Ether and Enamide under Irradiation: Scope, Mechanism, and The-oretical Elucidation of Hybrid Alkyl Pd(I)-Radical Species

Bin Zhao, Rui Shang, Guang-Zu Wang, Shaohong Wang, Hui Chen, and Yao Fu

ACS Catal., **Just Accepted Manuscript** • DOI: 10.1021/acscatal.9b04699 • Publication Date (Web): 19 Dec 2019

Palladium-Catalyzed Dual Ligand-Enabled Alkylation of Silyl Enol Ether and Enamide under Irradiation: Scope, Mechanism, and Theoretical Elucidation of Hybrid Alkyl Pd(I)-Radical Species

Bin Zhao,[1] Rui Shang,*[,1,2] Guang-Zu Wang,[1] Shaohong Wang,[3] Hui Chen,*[,3] and Yao Fu*[,1]

[1] Hefei National Laboratory for Physical Sciences at the Microscale, CAS Key Laboratory of Urban Pollutant Conversion, Anhui Province Key Laboratory of Biomass Clean Energy, iChEM, University of Science and Technology of China, Hefei, Anhui 230026, China.

[2] Department of Chemistry, The University of Tokyo, 7-3-1 Hongo, Bunkyo-ku, Tokyo 113-0033, Japan.

[3] Beijing National Laboratory for Molecular Sciences (BNLMS), CAS Key Laboratory of Photochemistry, CAS Research/Education Center for Excellence in Molecular Sciences, Institute of Chemistry, Chinese Academy of Sciences, Beijing 100190, China.

Supporting Information Placeholder

ABSTRACT: We report herein that a palladium catalyst in combination with a dual phosphine ligand system catalyzes alkylation of silyl enol ether and enamide with a broad scope of tertiary, secondary, and primary alkyl bromides under mild irradiation conditions by blue light-emitting diodes. The reactions effectively deliver α-alkylated ketones and α-alkylated N-acyl ketimines, it is difficult to prepare the latter by other methods in a stereoselective manner. The α-alkylated N-acyl ketimine products can be further subjected to chiral phosphoric acid-catalyzed asymmetric reduction with Hantzsch ester to deliver chiral N-acyl-protected α-arylated aliphatic amines in high enantioselectivity up to 99% ee, thus providing a method for facile synthesis of chiral α-arylated aliphatic amines, which are of importance in medicinal chemistry research. The N-acetyl ketimine product also reacted smoothly with various types of Grignard reagents to afford sterically bulky N-acetyl α-tertiary amines in high yields. Theoretical studies in combination with experimental investigation provide understanding of the reaction mechanism with respect to the dual ligand effect and the irradiation effect in the catalytic cycle. The reaction is suggested to proceed via a hybrid alkyl Pd(I)-radical species generated by inner-sphere electron transfer of phosphine-coordinated Pd(0) species with alkyl bromide. This intriguing hybrid alkyl Pd(I)-radical species is elucidated by theoretical calculation to be a triplet species coordinated by three phosphine atoms with a distorted tetrahedral geometry, and spinprohibition rather than metal-to-ligand charge transfer contributes to the kinetic stability of the hybrid alkyl Pd(I)-radical species to impede alkyl recombination to generate Pd(II) alkyl intermediate.

KEYWORDS: *Palladium • Alkylation • Silyl Enol Ether • Enamide • Hybrid Alkyl Pd(I)-Radical Species*

1. INTRODUCTION

With the easy availability of cheap light-emitting diodes,[1] the area of excited-state transition-metal catalysis[2] under visible light irradiation is attracting increasing attention and has seen substantial development in the synthetic community. After photoexcitation of a metal complex with visible light of certain wavelength, untapped reactivity that was distinct from known thermal reactivity could be discovered to enable new catalytic reactions. Recent studies have revealed that even the most popular and heavily explored palladium catalysts[3] exhibit a blend of radical and organometallic reactivity under irradiation by blue light-emitting diodes,[1,4] which suppresses the problematic β-H elimination step of alkyl-Pd(II) species to allow various alkylation reactions with broad scope.[5] These reactions were proposed to proceed through a putative hybrid alkyl Pd(I)-radical species,[6] which remains more elusive than the well-defined palladium intermediates[7] generated under thermal conditions.

With our continuing research interest in exploring palladium catalysis under visible light excitation,[5,8] we believe that understanding the ligand configuration and reactivity control of hybrid alkyl Pd(I)-radical species will facilitate discovery of new reactivity. We note that in many recent reports of excitation-state palladium catalysis, phosphine ligand was used in a much larger ratio to palladium salts in the optimized reaction conditions compared with the situation of thermal palladium catalysis,[9] despite the sacrificial amount necessary to reduce Pd(II) to Pd(0). Shang and colleagues also discovered that applying a dual ligand is sometimes crucial for the reactivity of excitation-state palladium catalysis,[5] which differs from the ligand requirement in thermal palladium catalysis. We rationalized the intermediate to be a dual phosphine ligand coordinated palladium(0) species to undergo irradiation-induced inner-sphere electron transfer (ISET) to generate a hybrid alkyl Pd(I)-radical species, which may be in equilibrium with alkyl Pd(II) species[4,10] through dissociation of the monodentate phosphine ligand (Figure 1A).[8d] We hypothesized that this reactivity of palladium species can be used for the alkylations (especially tertiary alkylation) of silyl enol ether[11] and N-acyl enamide[12] to deliver α-alkylated ketone and α-alkylated N-acyl ketimine through a blend of radical and organometallic reactivity (Figure 1B). Alkylation of N-acyl enamide with alkyl bromide to generate α-alkylate N-acyl imine, which is a useful intermediate for further reduction or addition to deliver primary amine after easy removal of N-acyl protection, has not been successfully achieved. N-acyl-protected imines appear to be

difficult to prepare from the corresponding ketones, especially in a stereospecific manner.[13]

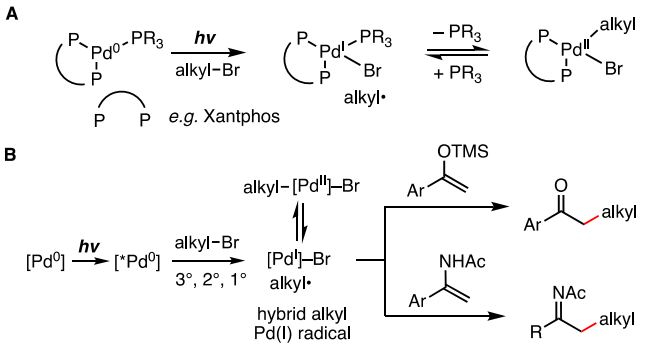

Figure 1. Working hypothesis of visible-light-induced palladium-catalyzed synthesis of α-alkylated ketone and imine via a hybrid alkyl Pd(I)-radical species

We report herein that by using excited-state reactivity of palladium catalyst in combination with two types of phosphine ligands (Xantphos and PPh_3) under irradiation of blue LEDs at room temperature, alkylations of silyl enol ether and N-acyl enamide were achieved with a broad scope of alkyl bromides including all tertiary, secondary, and primary alkyls. Theoretical study suggested that the reaction proceeds by irradiation-induced ISET from dual phosphine-coordinated Pd(0) to activate alkyl bromides to generate hybrid alkyl Pd(I)-radical species followed by a process involving dissociation and association of monodentate phosphine.[8d] The ligand structure and energy profiles of the intriguing hybrid alkyl Pd(I)-radical species are elucidated. The results presented here offer synthetic methods for preparation of α-alkylated ketone, α-alkylated N-acetyl ketimines, and enantiomerically pure α-arylated aliphatic amines. The theoretical explanation of the mechanism with respect to irradiation effect, dual ligand effect, and the structure of hybrid alkyl Pd(I)-radical species provides further guidance to design and explore palladium catalysis under irradiation excitation.

2. RESULTS AND DISCUSSION

2.1. Alkylation of Silyl Enol Ether and Enamide

The optimized reaction conditions for alkylation of trimethyl((1-phenylvinyl)oxy)silane and N-(1-phenylvinyl)acetamide with *tert*-butyl bromide are shown in Table 1. For alkylation of silyl enol ether, a combination of $Pd(PPh_3)_4$ (5 mol %) and Xantphos (6 mol %) served as the optimal catalyst to deliver the desired ketone product in 86% isolated yield after silica gel column chromatography. Notably, the Heck-type product was isolated in the absence of water using anhydrous dioxane. Water (10 equiv) was added to hydrolyze the alkylated silyl enol ether in situ to afford the ketone product. Dioxane was found to be the optimal solvent (see Supporting Information for results of screening solvents), and potassium acetate was found to be a mild base to trap the trimethylsilyl group. The palladium catalyst and irradiation by blue LEDs were essential for the reaction (entries 1 and 6 in Table 1A). The reaction proceeded in only 18% yield in the absence of Xantphos (entry 2, in Table 1A). Using $Pd(OAc)_2$ (5 mol %) and Xantphos (12 mol %) instead of $Pd(PPh_3)_4$ shut down the reactivity, revealing the essential role of the dual phosphine ligand system (entry 3, in Table 1A). $Pd_2(dba)_3$ (2.5 mol %) used instead of $Pd(PPh_3)_4$ was not productive (entry 4, in Table 1A). KOAc as base is also crucial for the reaction to proceed (entry 5, in Table 1A). Other bidentate phosphine ligands such as DPE-Phos, dppp, dppen, and triphos were all ineffective (Table 1A, bottom).

For alkylation of enamide shown in Table 1B, the optimal condition uses $Pd(OTfa)_2$ (5 mol %) as palladium source, and PPh_3 (12 mol %) and Xantphos (6 mol %) as the dual phosphine ligand system to afford the desired N-acyl ketimine in 96% isolated yield as single *E*-stereoisomer. The palladium catalyst, dual phosphine ligand, base, and irradiation were all essential parameters (entries 1–5, in Table 1B). Using a single phosphine ligand system containing the same amount of coordinative phosphine atoms composed of either PPh_3 (20 mol %) or Xantphos (12 mol %) was ineffective (entries 6 and 7, in Table 1B).

Table 1. Key Parameters Controlling Tertiary Alkylation of Silyl Enol Ether and Enamide[a]

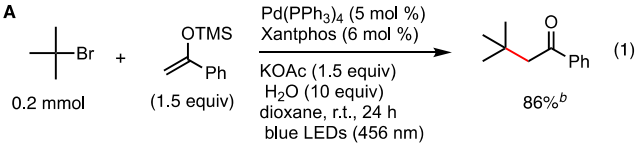

entry	*variation from standard condition*	yield (%)[c]
1	without $Pd(PPh_3)_4$	0
2	without Xantphos	18
3	$Pd(OAc)_2$ (5 mol %)/Xantphos (12 mol %) instead of $Pd(PPh_3)_4$ (5 mol %)	trace
4	$Pd_2(dba)_3$ (2.5 mol %) instead of $Pd(PPh_3)_4$ (5 mol %)	< 5%
5	without KOAc	0
6	without H_2O (10 equiv)	35
7	without irradiation	0

other phosphines (6 mol %) instead of Xantphos (6 mol %)

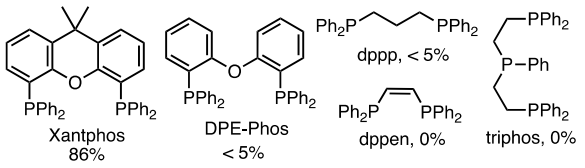

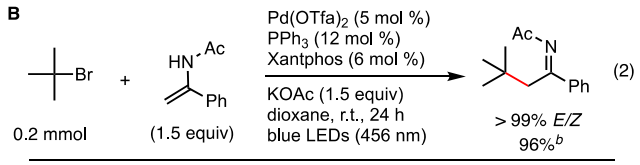

entry	*variation from standard condition*	yield (%)[c]
1	without $Pd(OTfa)_2$	0
2	without PPh_3	0
3	without Xantphos	0
4	without KOAc	0
5	without irradiation	0
6	PPh_3 (24 mol %) instead of PPh_3 (12 mol %) + Xantphos (6 mol %)	trace
7	Xantphos (12 mol %) instead of PPh_3 (12 mol %) + Xantphos (6 mol %)	trace

[a]Reaction performed at room temperature (25 ± 3 ° C) for 24 h under argon atmosphere. [b]Yield of isolated product. [c]Yield determined by ^{1}H-NMR using diphenylmethane as an internal standard.

The optimized reaction conditions for alkylation of silyl enol ether and enamide were applicable for a broad scope of substrates. The reaction scope with respect to alkylation of silyl enol ether is shown in Scheme 1. A broad scope of tertiary and secondary alkyl bromides including both cyclic and acyclic ones exhibited as amenable substrates **(1–14)**. Primary alkyl bromide **(15)** and benzyl bromide **(16)** were also suitable substrates. The reaction

is compatible with various functional groups and substituents such as ester **(4)**, alkyl chloride **(8)**, amide **(12)**, ether **(18)**, trifluoromethyl **(19)**, cyano **(21)**, aryl pinacol boronate **(22)**, and sulfone **(24)**. Both electron-rich **(18)** and electron-deficient **(19, 24, 28)** silyl enol ethers exhibited as suitable substrates. However, this reaction scope was limited to silyl enol ether derived from aromatic and heteroaromatic ketones **(29, 30)**. Silyl enol ether derived from aliphatic ketones was an incompatible substrate. Silyl enol ether derived from benzylideneacetone afforded the desired product in moderate yield **(31)**. Sily enol ethers derived from α-substituted acetophenones, (*e.g.* propiophenone) were not successful probably because of the increased steric hindrance.

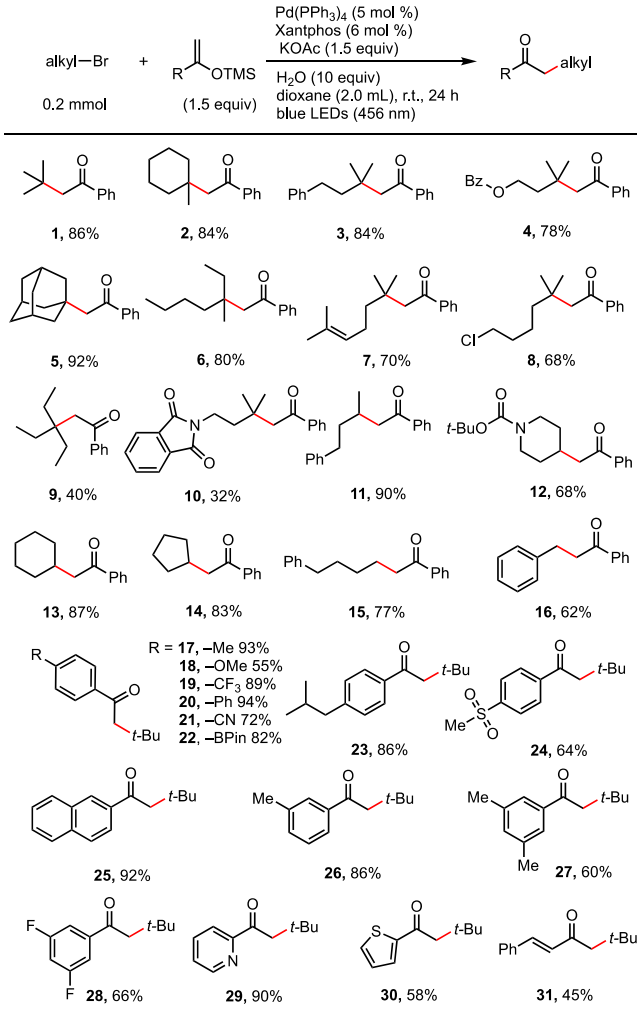

[a]Reaction conditions: alkyl halide (0.2 mmol), silyl enol ether (0.3 mmol), $Pd(PPh_3)_4$ (5 mol %), Xantphos (6 mol %), KOAc (150 mol %), 1,4-dioxane (2 mL), H_2O (2.0 mmol), irradiation by blue LEDs (456 nm) at room temperature for 24 h under argon atmosphere. Yield of isolated product.

Scheme 1. Scope of Alkylation of Silyl Enol Ether for Synthesis of α-Alkylated Ketones[a]

Tertiary alkylation can also be achieved using N-(acyloxy)phthamide by slightly modifying the ligand system to use Ni-Xantphos (eq. 3). However, because of the existence of a much cheaper and more efficient reaction system using NaI/PPh_3 developed previously,[14] we did not expand further the scope using the palladium system reported herein.

The synthetic value of this excited-state palladium-catalysis is highlighted by the synthesis of a broad scope of N-acyl-protected ketimines from N-acyl enamides and alkyl bromides. N-acyl-protected ketimines can be further (enantioselectively) reduced to afford primary amine, which is a class of useful intermediates for synthesis of bioactive compounds. Synthesis of N-acyl-protected ketimine is challenging because of the weak nucleophilicity of amide to condense with ketone. In addition, there is no efficient synthetic method to access stereochemically pure N-acyl ketimine. One study reported an isomerization-free method to access N-acyl imines from hazardous secondary azides under light irradiation,[15] but the compatibility of this method for the synthesis of α-alkylated ketimines with large steric hindrance was not demonstrated.

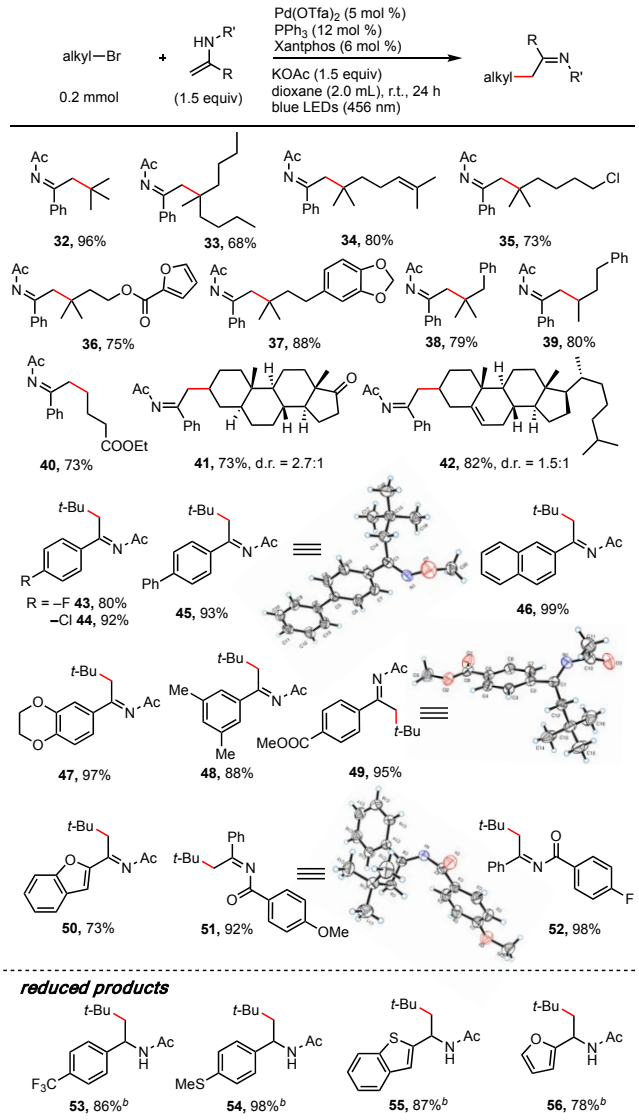

[a]Reaction conditions: alkyl halide (0.2 mmol), enamide (0.3 mmol), $Pd(OTfa)_2$ (5 mol %), PPh_3 (12 mol %), Xantphos (6 mol %), KOAc (150 mol %), 1,4-dioxane (2 mL), irradiation by blue LEDs (456 nm) at room temperature for 24 h under argon atmosphere. Yield of isolated product. Ratio of diastereomer measured by ^{1}H-NMR analysis. [b]Yield of isolated product obtained after in situ reduction using $NaBH_4$ (0.4 mmol) and acetic acid (0.6 mmol) at room temperature for 3 h.

Scheme 2. Reaction Scope of Stereoselective Synthesis of α-Alkylated Imines[a]

Our method using irradiation-induced palladium catalysis afforded a broad scope of α-tertiary, secondary, and primary alkylated N-acyl ketimines as pure stereoisomer (Scheme 2). The geometric structure of the stereoisomer was determined to be *E*-configuration by measuring single crystals of several products **(45, 49, 51)**. The reaction is applicable to complicated steroid-derived alkyl bromides to install imine functionality into steroid derivatives **(41, 42)**. Besides acetyl-protected ketimine, the reaction also afforded ketimines protected by both electron-rich and electron-deficient aroyl groups **(51, 52)**. The generated ketimine product can be in situ reduced by adding sodium borohydride and acetic acid at room temperature to deliver α-arylated aliphatic amines. Most importantly, α-alkylated N-acyl ketimine products can be subjected to chiral phosphoric acid-catalyzed asymmetric reduction[16] with Hantzsch ester to deliver α-arylated aliphatic amines in high enantioselectivity up to 99% ee, providing a new method for facile synthesis of chiral α-arylated aliphatic amines of structure diversity (Scheme 3). Although methods of chiral phosphoric acid-catalyzed enantioselective reduction of imine have been reported,[16a,17] they reports mostly used N-*p*-methoxyphenyl (PMP)-protected imines, which need further oxidation for deprotection. Moreover, the substrates in these reports were limited to ketimines derived from acetophenone derivatives,[16a, 17a] probably because of the synthetic complexity of accessing α-alkylated 1-arylethan-1-imine with structure diversity.

2.2. Further Transformation of α-Alkylated N-acyl Ketimine Products

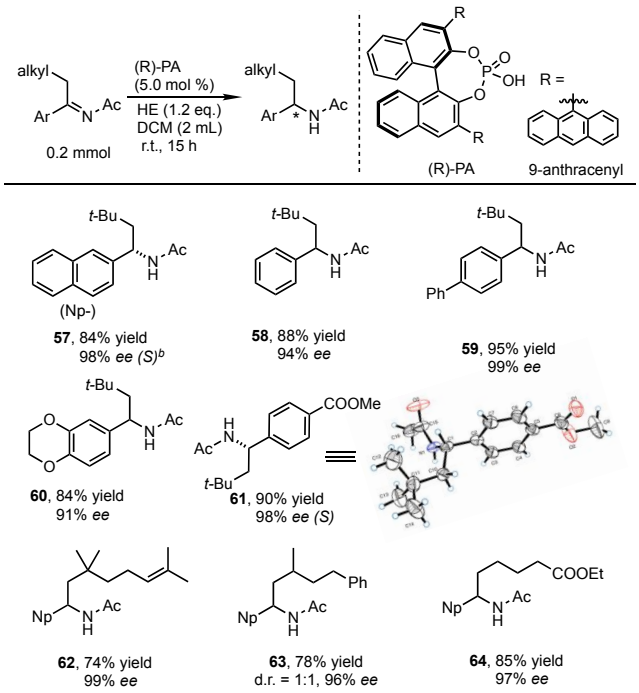

[a]Reaction conditions: imine (0.2 mmol), (*R*)-PA (5 mol %, 0.01 mmol), Hantzsch ester (120 mol %, 0.24 mmol), dichloromethane (2 mL). Yield of isolated product. Condition for determination of enantiomeric excess: HPLC, Daicel CHIRALPAK AD, hexane/2-propanol = 100/5 ~ 100/10, flow rate 1.0 mL/min. [b]Single crystal data shown in Supporting Information (Table S9). (*R*)-isomer was obtained in 82% isolated yield and 98% ee. when (*S*)-PA was used as catalyst.

Scheme 3. Chiral Phosphoric Acid-Catalyzed Enantioselective Reduction of N-Acyl Imine[a]

As shown in Scheme 3, α-tertiary alkylated ketimines **(57–62)**, α-secondary alkylated ketimine **(63)**, and α-primary alkylated ketimine **(64)** were all amenable substrates for asymmetric reduction to afford 2-arylated N-acetyl aliphatic amines in good yield and high enantioselectivity. Functional groups such as alkene **(62)** and ester **(61, 64)** did not affect the high enantioselectivity. When (*R*)-PA was used as catalyst, the absolute configuration of product **(57)** and **(61)** was determined to be (*S*)-configuration by X-ray crystallography. Changing the absolute configuration of chiral phosphoric acid catalyst resulted in inversion of the absolute configuration of the product with little effect on reaction efficiency **(57)**. These N-acetyl amines obtained in high ee and high yield are easily subjected to hydrolysis to give free amine. Also, the N-acetyl ketimine product reacted smoothly with various types of Grignard reagents, including methyl **(65)**, vinyl **(66)**, benzyl **(67)**, allyl **(68)**, phenyl **(69)**, cyclohexyl **(70)**, and isopropyl **(71)**, to afford sterically bulky N-acetyl α-tertiary amines in high yields (Scheme 4).[18]

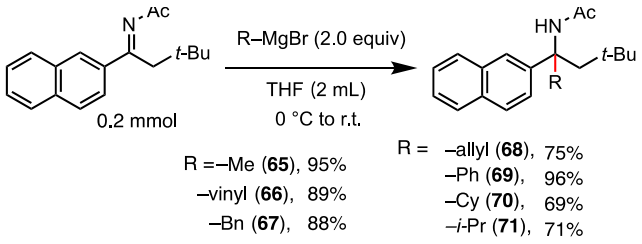

[a]Reaction conditions: imine (0.2 mmol), Grignard reagent (200 mol % in THF). Yield of isolated product.

Scheme 4. Synthesis of N-Acetyl α-Tertiary amines from N-acyl Ketimine Products[a]

2.3. Possible Mechanism of the Reaction with Dual Ligand Cooperation

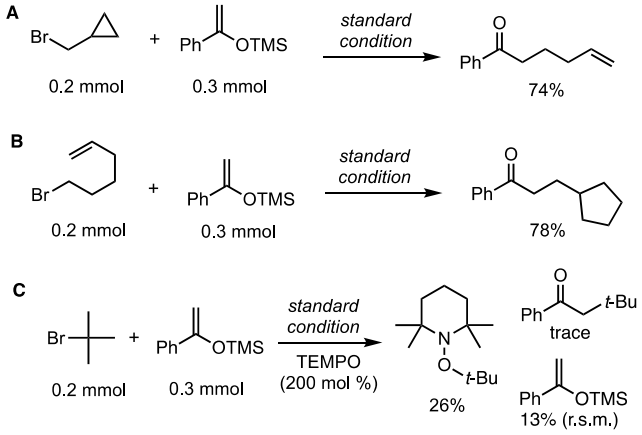

Scheme 5. Radical-Clock and Radical-Trapping Experiments

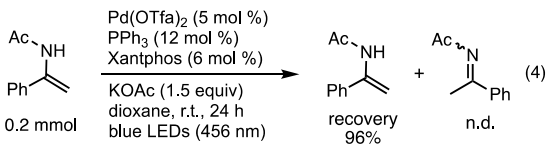

Although new catalytic reactivity of excited-state palladium species for alkyl cross-coupling[4,5,8] and C–H functionalization[19] has been reported by several research groups recently, the reactive alkyl palladium species under light irradiation remains elusive. It has been claimed that catalyst under visible light irradiation resembles a photoredox catalyst[20] applied in recently popularized photoredox chemistry.[21] A Recent theoretical study by Rueping and Cavallo[22] and a mechanistic investigation by Shang and colleagues[5,8] suggest that an ISET process between three phosphine-atom-coordinated Pd(0) species and alkyl electrophiles (alkyl bromide, or alkyl carboxylic acid N-hydroxyphthalimide ester) to generate hybrid alkyl Pd(I)-radical followed by ligand dissociation and association processes is more plausible. Through radical clock experiments[23] (Scheme 5A and 5B) and radical-trapping experiment using TEMPO as scavenger (Scheme 5C), the alkyl radical property of the intermediate was confirmed. For enamide reaction, a control experiment showed that enamide starting material did not isomerize to imine under the standard reaction condition (eq. 4). We propose a reaction mechanism that rationalizes the irradiation effect as well as the essential dual ligand effect in Figure 2. As shown, the reaction starts with photoactivation of a Pd(0) species three-coordinated by two phosphine ligands **(I)**. Visible light activation of **I** results in ISET to activate alkyl bromide to generate hybrid alkyl Pd(I)-radical species (**II**). Intermediate **II** reacts with silyl enol ether or enamide to generate benzylic type radical, which has stronger coordination ability toward palladium compared with saturated alkyls to replace a monodentate phosphine ligand to generate intermediate **IV**, on which β-H elimination proceeds to give intermediate **V**. Regeneration of **I** proceeds through association of monodentate phosphine ligand to release product. DFT calculation is further used to prove the possible reaction mechanism (Figure 3) and elucidate the nature of the intriguing hybrid alkyl Pd(I)-radical species (Figures 4–6).

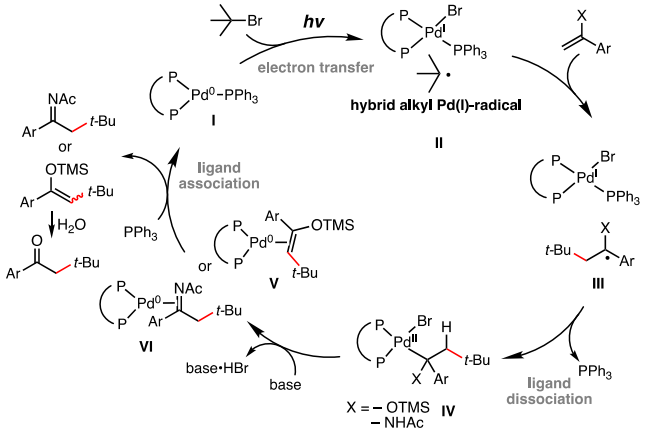

Figure 2. Proposed catalytic cycle.

DFT calculations[24] to support the proposed mechanism of alkylation between enamine **(a)** and *tert*-butyl bromide **(B)** are shown in Figure 3. In situ generated three-coordinated Pd^0(Xantphos)(PPh_3) **(A)** complex is considered as the reference structure for calculation. It is known that the phosphine-coordinated Pd(0) species needs to overcome a high energy barrier to undergo oxidative addition with tertiary alkyl bromide through a three-centered transition state that resembles oxidative addition with aryl halides.[25] Activation of *tert*-butyl bromide **(B)** through photoinduced ISET from **A** to generate ionized species **(A1+B1)** requires overcoming an energy barrier of 57.9 kcal/mol, an energy lower than the photon energy blue LEDs can provide (*approx.* 62.7 kcal/mol). DFT calculation and Marcus theory[26] were applied to compare the energy barriers for ISET from different Pd(0) species to **B**, and the results revealed that **A** has the lowest energy barrier (ΔG = 57.9 kcal/mol, ΔG^* = 58.3 kcal/mol) to activate **B**, while Pd^0(Xantphos) **(A′)** and $Pd^0(PPh_3)_3$ **(A″)** have higher energy barriers (ΔG = 68.7 kcal/mol, ΔG^* = 70.4 kcal/mol for **A′** and ΔG = 58.8 kcal/mol, ΔG^* = 59.2 kcal/mol for **A″**; see inset in Figure 3). These calculation results support that a Pd(0) species coordinated by three phosphine atoms is responsible for the ET process. Considering that ISET from **A** and **A″** to **B** overcomes similar energy barriers, the different outcomes using Xantphos/PPh_3 dual ligand and PPh_3 alone could be attributed to a better effect of Xantphos to stabilize hybrid alkyl Pd(I)-radical species compared with PPh_3 (cf. Figure 6A and 6C) . Fragmentation of **A1+B1** resulted in formation of hybrid alkyl Pd(I)-radical **(C+D)** with energy release of 40.3 kcal/mol. **C+D** further overcomes a small energy barrier to react with enamide to generate **C+E** by releasing energy of 16.4 kcal/mol. The two doublet species **C** and **E** collapse into a Pd(II) species **G** by dissociating PPh_3 ligand. This ligand dissociation process has an energy barrier of 17.2 kcal/mol. Further exchange of bromide by acetate generates **H** and β-H elimination gives imine-coordinated Pd(0) species. PPh_3 association to Pd(0) liberates the imine product and regenerates triphosphine-coordinated Pd(0) species **A** for the next catalytic cycle. Control calculation revealed that the generation of *E*-ketimine is thermodynamically favored by 0.6 kcal/mol, which explains the observed *E*-selectivity. A control experiment testing compound **32** under standard reaction condition without addition of alkyl bromide showed no stereoisomerization of *E*-ketimine, revealing no palladium-catalyzed E/Z isomerization. The whole catalytic cycle proceeds with a thermochemistry of the reaction **A (S_0) + B + a + KOAc → A (S_0) + c + KBr + HOAc,** which equals –7.2 kcal/mol. Besides the photoinduced ISET step, the energy barriers of all the other steps in the catalytic cycle are lower than 20 kcal/mol, which is in accordance with the room temperature condition. Irradiation plays an essential role in inducing ISET from Pd(0) to activate alkyl bromide.

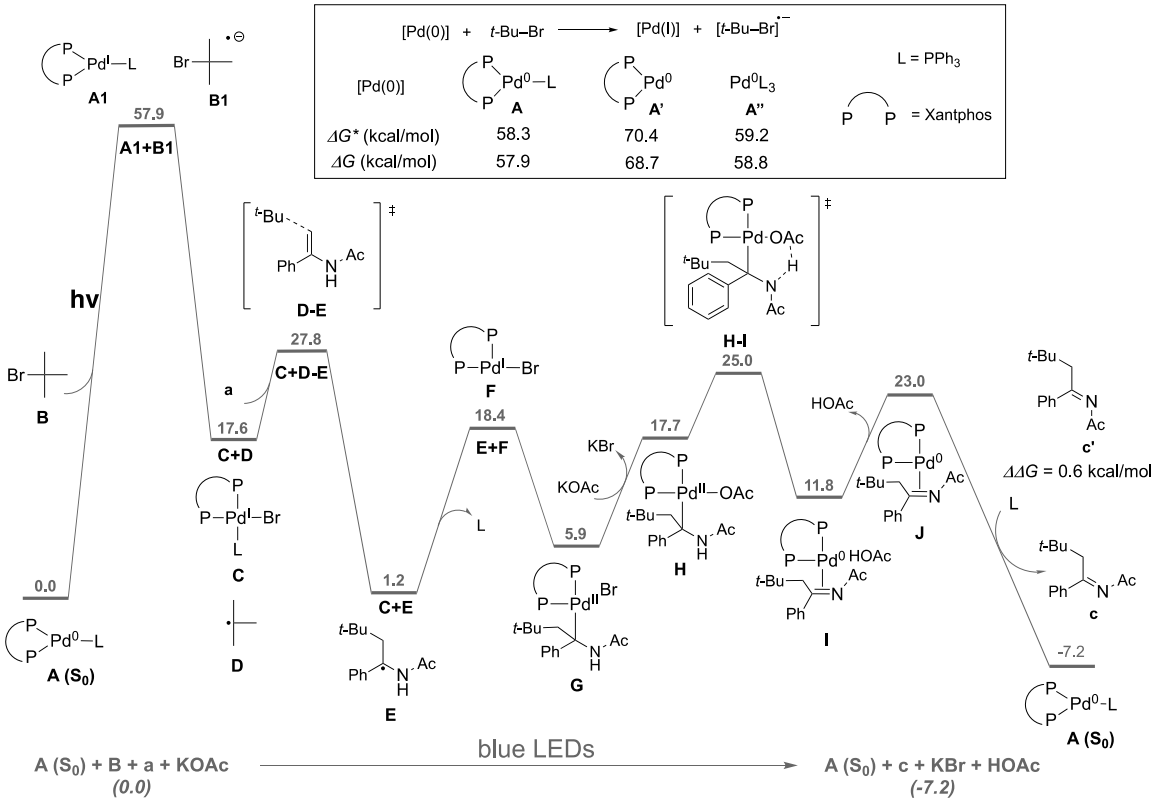

Figure 3. Computed energy profile for alkylation of enamide. Free energies in solution (in kcal/mol) at the M06/6-311+G(d,p)-SDD-SMD(Dioxane)//B3LYP/6-31G(d)-LANL2DZ level are displayed.

2.4. Theoretical Elucidation of Hybrid Alkyl Pd(I)-Radical Species

(1) The transformation between alkyl-Pd(II) and hybrid alkyl Pd(I)-radical

After clarifying the energy profile of the proposed reaction mechanism, theoretical calculation was used to elucidate the intriguing hybrid alkyl Pd(I)-radical species (**C**+**D** in Figure 3). The existence of this species in irradiation-induced palladium catalysis has been proposed, but was sometimes challenged because of the high propensity of alkyl radical recombination to a d^9 metal center. We consider that three factors may contribute to stabilizing this species to prevent alkyl recombination, 1) the dual ligand system, 2) a possible MLCT to ligand under irradiation, and 3) spin prohibition. DFT and TD-DFT calculations were used to clarify these issues. As shown in Figure 4, the transformation between alkyl-Pd(II) species (**K**) and hybrid alkyl Pd(I)-radical **(M)** species is a stepwise process involving **L** as intermediate, namely first dissociation of PPh_3 and then association with *t*-Bu•. The alkyl-Pd(II) species **K** and hybrid alkyl Pd(I)-radical **M** have very close stability, and the energy difference between them is only 0.6 kcal/mol. The barrier for transformation between **K** and **M** is relatively small (about 6–7 kcal/mol), indicating the kinetic easiness of this transformation.

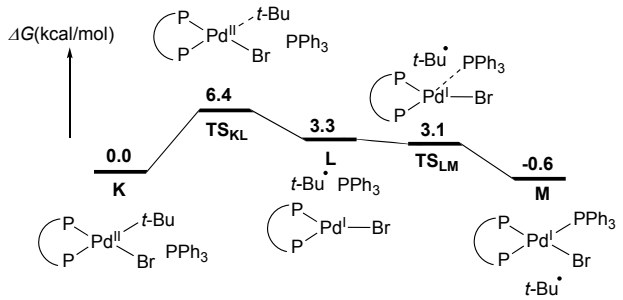

Figure 4. Transformation energy profile between alkyl-Pd(II) (**K**) and hybrid alkyl Pd(I)-radical species (**M**).

(2) The possibility of MLCT state for Xantphos-Pd(I)-PPh_3-Br

The possibility of MLCT between Xantphos and palladium center to stabilize Xantphos-Pd(I)-PPh_3-Br species was examined by DFT calculations. We first attempted to obtain this MLCT state in ground state DFT calculations. After swapping the orbitals for getting the proper MLCT configuration of Xantphos-Pd(I)-PPh_3-Br as input for DFT calculation, we found that it was impossible to obtain this MLCT state as the ground state, and the ligand π^* orbital of Xantphos was much higher in energy than the *d*-orbital of Pd(I). This explains why the MLCT state cannot be obtained in ground-state DFT calculations. We also tried TD-DFT calculations, and found that the MLCT state was an excited state that was much higher in energy than the ground state by 72.6 kcal/mol, an energy even higher than the energy of irradiation photons (Figure 5), Therefore, the MLCT state for Pd(I) species is unlikely to be involved in the catalytic cycle. Based on the calculated energies, we excluded the possibility of MLCT between Xantphos and Pd(I) contributing to stabilize the hybrid alkyl Pd(I)-radical species.

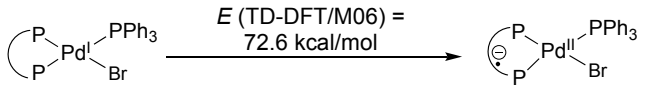

Figure 5. TD-DFT calculation to locate the MLCT state for Xantphos-Pd(I)-PPh_3-Br species.

(3) The possibility of spin prohibition to enhance the kinetic stability of hybrid alkyl Pd(I)-radical species (M)

As shown in Figure 4, with singlet hybrid alkyl Pd(I)-radical species **M,** it is kinetically easy to form alkyl-Pd(II) species. However, we found that triplet-state hybrid alkyl Pd(I)-radical species **M(triplet)** is slightly more stable than the singlet one (Figure 6A). In the triplet state, the formation of alkyl-Pd(II) species from **M(triplet)** is not feasible, and geometry optimization of alkyl-Pd(II) structure leads to spontaneous cleavage of the Pd–C bond and release of *t*-Bu•. Therefore, it is possible for M(triplet) to serve as a kinetically more stable form of hybrid alkyl Pd(I)-radical species that has a longer lifetime. The optimized structure and electron distribution of **M(triplet)** are shown in Figure 6B, where the Pd(I) center is coordinated by three phosphine atoms with a distorted tetrahedral geometry. Based on these results, we also investigated the energy difference between Xantphos-Pd(I)-PPh_3-Br/*t*-Bu• intermediate (**M**) and Pd(I)-$(PPh_3)_3$-Br/*t*-Bu• intermediate to understand the essential effect of Xantphos as ligand (Figure 6C). As shown in Figure 6C, Pd(I)-$(PPh_3)_3$-Br/*t*-Bu• intermediate is +5.8 kcal/mol higher in energy compared with alkyl-recombined Pd(II) intermediate **K′**. The triplet state of **M′** is +5.1 kcal/mol higher in energy compared with **K′**.

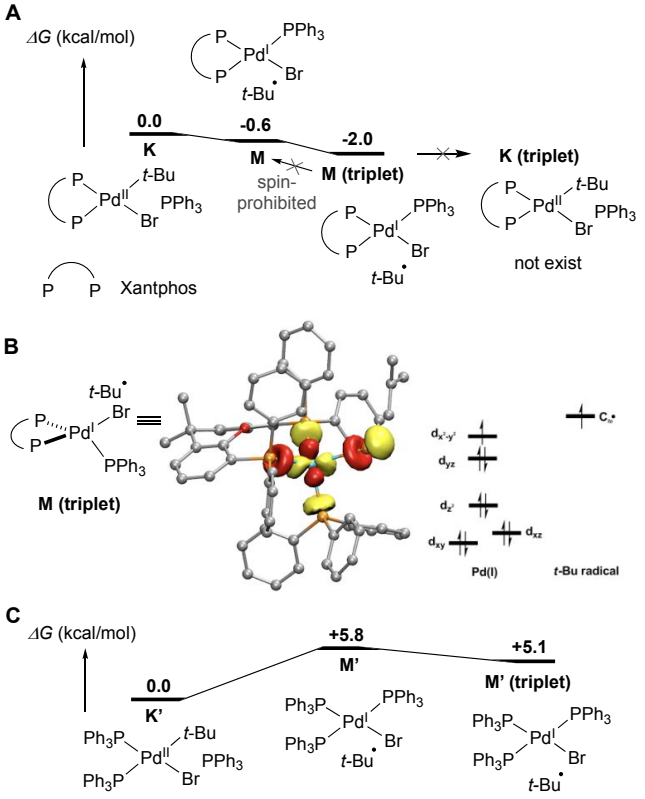

Figure 6. The triplet **M(triplet)** as a more stable hybrid alkyl Pd(I)-radical species (**M**) to avoid the kinetically active singlet **M**. (A) The Spin-Prohibition effect to kinetically stabilize triplet hybrid alkyl Pd(I)-radical species. (B) Computed structure and *d*-orbital electron distribution of triplet hybrid alkyl Pd(I)-radical species. Orbitals indicating spin delocalization on Pd(I) radical species. (C) Eneries of singlet and triplet states of Pd(I)-$(PPh_3)_3$-Br/*t*-Bu• (M′) compared with K′.

These calculation results shown in Figure 6A and Figure 6C revealed that Xantphos facilitates the formation of hybrid alkyl Pd(I)-radical species, which explains the essential role of Xantphos for these reactions.

Based on the above calculations, we conclude that Xantphos-ligated hybrid alkyl Pd(I)-radical species (**M**) is thermodynamically more favorable compared with alkyl-recombined Pd(II) species (**K**), and spin prohibition rather than MLCT contributes to the kinetic stability of **M** to impede alkyl recombination.

3. CONCLUSION

In summary, alkylation of silyl enol ether and enamide with tertiary, secondary, and primary alkyl bromides was achieved using visible-light-induced palladium catalysis applying a dual phosphine ligand system. The reactions effectively deliver α-alkylated ketones, as well as α-alkylated N-acyl ketimine in a stereoselective manner. The α-alkylated N-acyl ketimine products can be subjected to chiral phosphoric acid-catalyzed asymmetric reduction with Hantzsch ester to deliver chiral α-arylated N-acyl-protected aliphatic amines in high enantioselectivity up to 99% ee. The N-acetyl ketimine products also reacted with various Grignard reagents to produce N-acetyl α-tertiary amines in good yields. Theoretical studies provided mechanistic understanding of the reaction mechanism with respect to the dual ligand effect and irradiation effect in the catalytic cycle. The reaction is suggested to proceed via a hybrid alkyl Pd(I)-radical species generated by ISET from dual phosphine ligand-coordinated Pd(0) species to alkyl bromide. This intriguing hybrid alkyl Pd(I)-radical species was elucidated by theoretical calculation to be a triplet species coordinated by three phosphine atoms with a distorted tetrahedral geometry, which is energetically slightly favored compared with the corresponding alkyl-recombined Pd(II) species. Spin prohibition rather than MLCT contributes to the stability of hybrid alkyl Pd(I)-radical species to impede alkyl recombination. The discovered reactions add examples to the repertoire of excited-state palladium catalysis. It is hoped that the theoretically elucidated structure and reactivity of hybrid alkyl Pd(I)-radical species as well as the dual ligand effect will provide guidance in related fields for the discovery of new reactivity of excited-state transition metal catalysis under visible light.

ASSOCIATED CONTENT

AUTHOR INFORMATION

Corresponding Authors

*E-mail: rui@chem.s.u-tokyo.ac.jp (R.S.); chenh@iccas.ac.cn (H.C.); fuyao@ustc.edu.cn (Y. F.)

Notes

The authors declare no competing financial interest.

Supporting Information

This material is available free of charge via the Internet at http://pubs.acs.org.
Experimental details and characterization data for all products (PDF).
Crystallographic data for **45** (CIF)
Crystallographic data for **49** (CIF)
Crystallographic data for **51** (CIF)
Crystallographic data for **57** (CIF)
Crystallographic data for **61** (CIF)

ACKNOWLEDGMENTS

This work was supported by National Key R&D Program of China (2018YFB1501600, 2017YFA0303502), National Natural Science Foundation of China (21572212, 21732006, 51821006, 51961135104, 21833011), Strategic Priority Research Program of CAS (XDB20000000, XDA21060101), HCPST (2017FXZY001), KY (2060000119). Calculations were conducted on the supercomputing system in the Supercomputing Center of USTC.

REFERENCES

(1) (a) Dollen, P. V.; Pimputkar, S.; Speck, J. S., Let There be Light-with Gallium Nitride: the 2014 Nobel Prize in Physics. *Angew. Chem. Int. Ed.* **2014**, *53*, 13978–13980.

(2) (a) Creutz, S. E.; Lotito, K. J.; Fu, G. C.; Peters, J. C., Photoinduced Ullmann C-N Coupling: Demonstrating the Viability of a Radical Pathway. *Science* **2012**, *338*, 647–651. (b) Kainz, Q. M.; Matier, C. D.; Bartoszewicz, A.; Zultanski, S. L.; Peters, J. C.; Fu, G. C., Asymmetric Copper-catalyzed C-N Cross-couplings Induced by Visible Light. *Science* **2016**, *351*, 681–684. (c) Huang, L.; Rudolph, M. Rominger, F. Hashmi, A. S. K., Photosensitizer-free Visible-light-mediated Gold-catalyzed 1,2-Difunctionalization of Alkynes. *Angew. Chem. Int. Ed.* **2016**, *55*, 4808–4813. (d) Zhao, W.; Wurz, R. P.; Peters, J. C.; Fu, G. C., Photoinduced, Copper-catalyzed Decarboxylative C-N Coupling to Generate Protected Amines: an Alternative to the Curtius Rearrangement. *J. Am. Chem. Soc.* **2017**, *139*, 12153–12156. (e) Matier, C. D.; Schwaben, J.; Peters, J. C.; Fu, G. C., Copper-catalyzed Alkylation of Aliphatic Amines Induced by Visible Light. *J. Am. Chem. Soc.* **2017**, *139,* 17707–17710. (f) Ahn, J. M.; Peters, Peters, J. C.; Fu, G. C., Design of a Photoredox Catalyst that enables the Direct Synthesis of Carbamate-protected Primary Amines via Photoinduced, Copper-catalyzed N-alkylation Reactions of Unactivated Secondary Halides. *J. Am. Chem. Soc.* **2017***, 139,* 18101–18106. (g) Parasram, M.; Gevorgyan, V., Visible Light-induced Transition Metal-catalyzed Transformations: Beyond Conventional Photosensitizers. *Chem. Soc. Rev.* **2017**, *46*, 6227–6240. (h) Meng, Q.-Y.; Schirmer, T. E.; Katou, K.; König, B., Controllable Isomerization of Alkenes by Dual Visible-light-cobalt Catalysis. *Angew. Chem. Int. Ed.* **2019**, *58*, 5723–5278. (i) Schwarz, J.; König, B., Visible-light Mediated C-C Bond Cleavage of 1, 2-Diols to Carbonyls by Cerium-photocatalysis. *Chem. Commun.* **2019**, *55*, 486–488. (j) Kancherla, R.; Muralirajan, K.; Sagadevan, A.; Rueping, M., Visible Light-induced Excited-state Transition-metal Catalysis. *Trends Chem.* **2019,** *1*, 510–523.

(3) (a) Heck, R. F.; Nolley, J. P., Palladium-catalyzed Vinylic Hydrogen Substitution Reactions with Aryl, Benzyl, and Styryl Halides. *J. Org. Chem.* **1972**, *37*, 2320–2322. (b) King, A. O.; Okukado, N.; Negishi, E., Highly General Stereo-, Regio-, and Chemo-selective Synthesis of Terminal and Internal Conjugated Enynes by the Pd-catalysed Reaction of Alkynylzinc Reagents with Alkenyl Halides. *J. Chem. Soc., Chem. Commun.* **1977**, 683–684. (c) Miyaura, N.; Suzuki, A., Stereoselective Synthesis of Arylated (*E*)-alkenes by the Reaction of Alk-1-enylboranes with Aryl Halides in the Presence of Palladium Catalyst. *J. Chem. Soc., Chem. Commun.* **1979**, *19*, 866–867. (d) Jana, R.; Pathak, T. P.; Sigman, M. S., Advances in Transition Metal (Pd, Ni, Fe)-catalyzed Cross-coupling Reactions using Alkyl-organometallics as Reaction Partners. *Chem. Rev.* **2011**, *111*, 1417–1492. (e) Metal-catalyzed Cross-coupling Reactions and More; De Meijere, A., Brase, S., Oestreich, M., Eds.; Wiley-VCH: Weinheim, Germany, **2014**.

(4) (a) Parasram, M.; Chuentragool, P.; Sarkar, D.; Gevorgyan, V., Photoinduced Formation of Hybrid Aryl Pd-radical Species Capable of 1, 5-HAT: Selective Catalytic Oxidation of Silyl Ethers Into Silyl Enol Ethers. *J. Am. Chem. Soc.* **2016**, *138*, 6340–6343. (b) Parasram, M.; Chuentragool, P.; Wang, Y.; Shi, Y.; Gevorgyan, V., General, Auxiliary-enabled Photoinduced Pd-catalyzed Remote Desaturation of Aliphatic Alcohols. *J. Am. Chem. Soc.* **2017**, *139*, 14857–14860. (c) Chuentragool, P.; Parasram, M.; Shi, Y.; Gevorgyan, V., General, Mild, and Selective Method for Desaturation of Aliphatic Amines. *J. Am. Chem. Soc.* **2018**, *140*, 2465–2468. (d) Ratushnyy, M.; Parasram, M.; Wang, Y.; Gevorgyan, V., Palladium-catalyzed Atom-transfer Radical Cyclization at Remote Unactivated C(sp^3)-H Sites: Hydrogen-atom Transfer of Hybrid Vinyl Palladium Radical Intermediates. *Angew. Chem. Int. Ed.* **2018**, *57*, 2712–2715. (e) Chuentragool, P.; Kurandina, D.; Gevorgyan, V., Catalysis with Palladium Complexes Photoexcited by Visible Light. *Angew. Chem. Int. Ed.* **2019**, *58*, 11586–11598.

(5) (a) Wang, G.-Z.; Shang, R.; Cheng, W.-M.; Fu, Y., Irradiation-induced Heck Reaction of Unactivated Alkyl Halides at Room Temperature. *J. Am. Chem. Soc.* **2017**, *139*, 18307–18312. (b) Kurandina, D.; Parasram, M.; Gevorgyan, V., Visible Light-induced Room-temperature Heck Reaction of Functionalized Alkyl Halides with Vinyl Arenes/heteroarenes. *Angew. Chem. Int. Ed.* **2017**, *56*, 14212–14216. (c) Kurandina, D.; Rivas, M.; Radzhabov, M.; Gevorgyan, V., Heck Reaction of Electronically Diverse Tertiary Alkyl Halides. *Org. Lett.* **2018**, *20*, 357–360. (d) Wang, G.-Z.; Shang, R.; Fu, Y., Irradiation-induced Palladium-catalyzed Direct C–H Alkylation of Heteroarenes with Tertiary and Secondary Alkyl Bromides. *Synthesis* **2018***, 50,* 2908–2914. (e) Koy, M.; Sandfort, F.; Tlahuext-Aca, A.; Quach, L.; Daniliuc, C. G.; Glorius, F. Palladium-catalyzed Decarboxylative Heck-type Coupling of Activated Aliphatic Carboxylic Acids Enabled by Visible Light. *Chem. Eur. J.* **2018**, *24*, 4552–4555. (f) Koy, M.; Bellotti, P. Katzenburg, F.; Daniliuc, C. G.; Glorius, F. Synthesis of All-carbon Quaternary Centers by Palladium-catalyzed olefin Dicarbofunctionalization. *Angew. Chem. Int. Ed.* **2019**, 10.1002/anie.201911012. (g) Xing, W.-L.; Shang, R.; Wang, G.-Z.; Fu, Y. Visible Light-Induced Palladium-Catalyzed Ring Opening β-H Elimination and Addition of Cyclobutanone Oxime Esters. *Chem. Commun.* **2019,** *55,* 14291–14294.

(6) (a) Ariafard, A.; Lin, Z., Understanding the Relative Easiness of Oxidative Addition of Aryl and Alkyl Halides to Palladium(0). *Organometallics* **2006**, *25*, 4030–4033. (b) Seechurn, C. C. C. J.; Kitching, M. O.; Colacot, T. J.; Snieckus, V., Palladium-catalyzed Cross-coupling: A Historical Contextual Perspective to the 2010 Nobel Prize. *Angew. Chem. Int. Ed.* **2012**, *51*, 5062–5085. (c) Ruiz-Castillo, P.; Buchwald, S. L., Applications of Palladium-catalyzed C-N Cross-coupling Reactions. *Chem. Rev.* **2016**, *116*, 12564–12649. (d) Wang, C.; Dong, G., Direct β-alkylation of Ketones and Aldehydes via Pd-catalyzed Redox Cascade. *J. Am. Chem. Soc.* **2018**, *140*, 6057–6061. (e) Wang, C.; Rago, A. J.; Dong, G., Direct β-alkenylation of Ketones via Pd-catalyzed Redox Cascade. *Org. Lett*. **2019**, *21*, 3377–3381.

(7) (a) Hartwig, J. F., Transition-metal Catalyzed Synthesis of Arylamines and Aryl Ethers from Aryl Halides and Triflates: Scope and Mechanism. *Angew. Chem. Int. Ed.* **1998**, *37*, 2046–2067. (b) Culkin, D. A.; Hartwig, J. F., Palladium-catalyzed α-Arylation of Carbonyl Compounds and Nitriles. *Acc. Chem. Res*. **2003**, *36*, 234–245. (c) Hartwig, J. F., Evolution of a Fourth Generation Catalyst for the Amination and Thioetherification of Aryl Halides. *Acc. Chem. Res.* **2008**, *41*, 1534–1544. (d) Martin, R.; Buchwald, S. L., Palladium-catalyzed Suzuki-Miyaura Cross-coupling Reactions Employing Dialkylbiaryl Phosphine Ligands. *Acc. Chem. Res.* **2008**, *41*, 1461–1473. (e) Surry, D. S.; Buchwald, S. L., Biaryl Phosphane Ligands in Palladium-catalyzed Amination. *Angew. Chem. Int. Ed.* **2008**, *47*, 6338–6361. (f) Engle, K, M.; Mei, T.-S.; Wasa, M.; Yu, J.-Q., Weak Coordination as a Powerful Means for Developing Broadly Useful C–H Functionalization Reactions. *Acc. Chem. Res.* **2012**, 45, 788–802. (g) Shang, R.; Huang, Z.; Xiao, X.; Lu, X.; Fu, Y.; Liu, L., β-Aryl Nitrile Construction via Palladium-catalyzed Decarboxylative Benzylation of α-Cyano Aliphatic Carboxylate Salts. *Adv. Synth. Catal.* **2012**, *354*, 2465–2472. (h) Dong, Z.; Ren, Z.; Thompson, S. J.; Xu, Y.; Dong, G., Transition-metal-catalyzed C–H Alkylation using Alkenes. *Chem. Rev.* **2017**, *117*, 9333–9403. (i) Wang, J.; Dong, G., Palladium/norbornene Cooperative Catalysis. *Chem. Rev.* **2019,** *119*, 7478–7528.

(8) (a) Cheng, W.-M.; Shang, R.; Yu, H.-Z.; Fu, Y., Room-temperature Decarboxylative Couplings of α-Oxocarboxylates with Aryl Halides by Merging Photoredox with Palladium Catalysis. *Chem. Eur. J.* **2015**, *21*, 13191–13195. (b) Zhao, B.; Shang, R.; Cheng, W.-M.; Fu, Y., Decarboxylative Formylation of Aryl Halides with Glyoxylic Acid by Merging Organophotoredox with Palladium Catalysis. *Org. Chem. Front.* **2018**, *5*, 1782–1786. (c) Cheng, W.-M.; Shang, R.; Fu, Y., Irradiation-induced Palladium-catalyzed Decarboxylative Desaturation Enabled by a Dual Ligand System. *Nat. Commun.* **2018**, *9*, 5215. (d) Wang, G.-Z.; Shang, R.; Fu, Y., Irradiation-induced Palladium-catalyzed Decarboxylative Heck Reaction of Aliphatic N-(acyloxy)phthalimides at Room Temperature. *Org. Lett.* **2018**, *20*, 888–891. (e) Zheng, C.; Cheng, W.-M.; Li, H.-L. Na, R.-S.; Shang, R., *cis*-Selective Decarboxylative Alkenylation of Aliphatic Carboxylic Acids with Vinyl Arenes Enabled by Photoredox/palladium/uphill Triple Catalysis. *Org. Lett.* **2018**, *20*, 2559–2563.

(9) (a) Leeuwen, P. W. N. M.; Kamer, P. C. J.; Reek, J. N. H.; Dierkes, P., Ligand Bite Angle Effects in Metal-catalyzed C-C Bond Formation. *Chem. Rev.* **2000**, *100*, 2741–2769. (b) Shang, R.; Fu, Y.; Li, J.-B.; Zhang, S.-L.; Guo, Q.-X.; Liu, L., Synthesis of Aromatic Esters via Pd-catalyzed Decarboxylative Coupling of Potassium Oxalate Monoesters with Aryl Bromides and Chlorides. *J. Am. Chem. Soc.* **2009**, *131*, 5738–5739. (c) Birkholz (née Gensow), M.-N.; Freixab, Z.; Leeuwen, P. W. N. M., Bite Angle Effects of Diphosphines in C–C and C–X Bond Forming Cross Coupling Reactions. *Chem. Soc. Rev.* **2009**, *38*, 1099–1118. (d) Shang, R.; Yang, Z.-W.; Wang, Y.; Zhang, S.-L.; Liu, L., Palladium-Catalyzed Decarboxylative Couplings of 2-(2-Azaaryl)acetates with Aryl Halides and Triflates. *J. Am. Chem. Soc.* **2010**, *132*, 14391–14393. (e) Fernández-Pérez, H.; Etayo, P.; Panossian, A.; Vidal-Ferran, A., Phosphine-phosphinite and Phosphine-phosphite Ligands: Preparation and Applications in Asymmetric Catalysis. *Chem. Rev.* **2011**, *111*, 2119–2176. (f) Fischer, C.; Koenig, B., Palladium- and Copper-mediated N-Aryl Bond Formation Reactions for the Synthesis of Biological Active Compounds. *Beilstein J. Org. Chem.* **2011**, *7*, 59–74. (g) Huang, W.; Buchwald, S. L., Palladium-catalyzed N-arylation of Iminodibenzyls and Iminostilbenes with Aryl- and Heteroaryl halides. *Chem. Eur. J.* **2016**, *22*, 14186–14189. (h) Olsen, E. P. K.; Arrechea, P. L.; Buchwald, S. L., Mechanistic Insight Leads to A Ligand which Facilitates the Palladium-catalyzed Formation of 2-(Hetero)arylaminooxazoles and 4-(Hetero)arylaminothiazoles. *Angew. Chem. Int. Ed.* **2017**, *56*, 10569–10572. (i) Zhang, H.; Ruiz-Castillo, P.; Buchwald, S. L., Palladium-catalyzed C–O Cross-coupling of Primary Alcohols. *Org. Lett.* **2018**, *20*, 1580–1583. (j) Li, R.; Dong, G., Direct Annulation between Aryl Iodides and Epoxides through Palladium/norbornene Cooperative Catalysis. *Angew. Chem. Int. Ed*. **2018**, *57*, 1697–1701. (k) Jin, L.; Wang, J.; Dong, G., Palladium-catalyzed Ɣ-C(sp^3)-H Arylation of Thiols by a Detachable Protecting/directing Group. *Angew. Chem. Int. Ed.* **2018**, *57*, 12352–12355. (l) Li, R.; Liu, F.; Dong, G., Redox-neutral ortho Functionalization of Aryl Boroxines via Palladium/norbornene Cooperative Catalysis. *Chem* **2019**, *5*, 929–940.

(10) (a) Amatore, C.; Jutand, A., Anionic Pd(0) and Pd(II) Intermediates in Palladium-catalyzed Heck and Cross-coupling Reactions. *Acc. Chem. Res.* **2000**, *33*, 314–321. (b) Frisch, A. C.; Beller, M., Catalysts for Cross-coupling Reactions with Non-activated Alkyl Halides. *Angew. Chem. Int. Ed.* **2005**, *44*, 674–688. (c) Sargent, B. T.; Alexanian, E. J., Palladium-catalyzed Alkoxycarbonylation of Unactivated Secondary Alkyl Bromides at Low Pressure. *J. Am. Chem. Soc.* **2016**, *138*, 7520–7523.

(11) (a) Rasmussen, J. K., *O*-silylated Enolates-versatile Intermediates for Organic Synthesis. *Synthesis* **1977**, *2*, 91–110. (b) Reetz, M. T., Lewis Acid Induced α-Alkylation of Carbonyl Compounds. *Angew. Chem. Int. Ed.* **1982**, *21*, 96–108. (c) Brownbridge, P., Enol Ethers in Synthesis. *Synthesis* **1983**, *1*, 85–104. (d) Kuwajima, I.; Nakamura, E. Reactive Enolates from Enol Silyl Ethers. *Acc. Chem. Res.* **1985**, *18*, 181–187. (e) Evans, D. A.; Black, W. C., Total Synthesis of (+)-A83543A [(+)-Lepicidin A]. *J. Am. Chem. Soc.* **1993**, *115*, 4497–4513. (f) Johnson, C. R.; Raheja, R. K., Hydrosilylation of Enones: Platinum Divinyltetramethyldisiloxane Complex in the Preparation of Triisopropylsilyl and Triphenylsilyl Enol Ethers. *J. Org. Chem.* **1994**, *59*, 2287–2288. (g) Cahard, D.; Duhamel, P., Alkoxide-mediated Preparation of Enolates from Silyl Enol Ethers and Enol Acetates-from Discovery to Synthetic Applications. *Eur. J. Org. Chem.* **2001**, 1023–1031.

(12) (a) Hatakeyama, T.; Ito, S.; Nakamura, M.; Nakamura, E., Alkylation of Magnesium Enamide with Alkyl Chlorides and Fluorides. *J. Am. Chem. Soc.* **2005**, *127*, 14192–14193. (b) Zhao, H.; Vandenbossche, C. P.; Koenig, S. G. Singh, S. P.; Bakale, R. P., An Efficient Synthesis of Enamides from Ketones. *Org. Lett.* **2008**, *10*, 505–507. (c) Hesp, K. D.; Bergman, R. G.; Ellman J. A., Expedient Synthesis of N-acyl Anthranilamides and β-Enamine Amides by the Rh(III)-catalyzed Amidation of Aryl and Vinyl C–H Bonds with Isocyanates. *J. Am. Chem. Soc.* **2011**, *133*, 11430–11433. (d) Reeves, J. T.; Tan, Z.-L.; Han, Z. S.; Li, G.-S.; Zhang, Y.-D.; Xu, Y.-B.; Reeves, D. C.; Gonnella, N. C.; Ma, S.-L.; Lee, H.; Lu, B. Z.; Senanayake, C. H., Direct Titanium-mediated Conversion of Ketones into Enamides with Ammonia and Acetic Anhydride. *Angew. Chem. Int. Ed.* **2012**, *51*, 1400–1404.

(13) (a) Padwa, A.; Akiba, M.; Cohen, L. A.; MacDonald, J. G., Sigmatropic Rearrangements in the Allyl Substituted Oxazolinone System. *Tetrahedron Lett*. **1981**, *22*, 2435–2438. (b) Kupfer, R.; Meier, S.; Würthwein, E., A Facile Method for the Synthesis of Substituted *N*-Methylenecarboxamides and Alkyl *N*-Methylenecarbamates. *Synthesis* **1984**, *8*, 688–690. (c) Vidal, J.; Damestoy, S.; Guy, L.; Hannachi, J.; Aubry, A.; Collet, A., *N*-Alkyloxycarbonyl-3-aryloxaziridines: Their Preparation, Structure, and Utilization as Electrophilic Amination Reagents. *Chem. Eur. J.* **1997**, *3*, 1691–1709. (d) Matsuo, J.; Tanaki, Y.; Kido, A.; Ishibashi, H., A Mild and Convenient Synthesis of *N*-Carbobenzyloxy Ketimines. *Chem. Commun.* **2006**, 2896–2898. (e) Zanardi, A.; Mata, J. A.; Peris, E., One-pot Preparation of Imines from Nitroarenes by a Tandem Process with an Ir-Pd Heterodimetallic Catalyst. *Chem. Eur. J.* **2010**, *16*, 10502–10506. (f) Yin, B.; Zhang, Y.; Xu, L.-W., Recent Applications of α-Amido Sulfones as in situ Equivalents of Activated Imines for Asymmetric Catalytic Nucleophilic Addition Reactions. *Synthesis* **2010**, *21*, 3583–3595.

(14) Fu, M.-C.; Shang, R.; Zhao, B.; Wang, B.; Fu, Y., Photocatalytic Decarboxylative Alkylations Mediated by Triphenylphosphine and Sodium Iodide. *Science* **2019**, *363*, 1429–1434.

(15) Kwon, Y.; Rhee, Y. H.; Park, J., Chemoselective, Isomerization-free Synthesis of *N*-Scylketimines from N–H Imines. *Adv. Synth. Catal.* **2017**, *359*, 1503–1507.

(16) (a) Hoffmann, S.; Seayad, A. M.; List, B., A Powerful Brønsted Acid Catalyst for the Organocatalytic Asymmetric Transfer Hydrogenation of Imines. *Angew. Chem. Int. Ed.* **2005**, *44*, 7424–7427. (b) Wang, Z.; Ye, X.; Wei, S.; Wu, P.; Zhang, A.; Sun, J., A Highly Enantioselective Lewis Basic Organocatalyst for Reduction of *N*-Aryl Imines with Unprecedented Substrate Spectrum. *Org. Lett.* **2006**, *8*, 999–1001. (c) Li, G.; Liang, Y.; Antilla, J. C., A Vaulted Biaryl Phosphoric Acid-catalyzed Reduction of α-Imino Esters: the Highly Enantioselective Preparation of α-Amino Esters. *J. Am. Chem. Soc.* **2007**, *129*, 5830–5831. (d) You, S.-L., Recent Developments in Asymmetric Transfer Hydrogenation with Hantzsch Esters: a Biomimetic Approach. *Chem. Asian J.* **2007**, *2*, 820–827. (e) Pei, D.; Zhang, Y.; Wei, S. Y.; Wang, M.; Sun, J., Rationally-Designed *S*-chiral Bissulfinamides as Highly Enantioselective Organocatalysts for Reduction of Ketimines. *Adv. Synth. Catal.* **2008**, *350*, 619–623. (f) Guizzetti, S.; Benaglia, M.; Rossi, S., Highly Stereoselective Metal-free Catalytic Reduction of Imines: an Easy Entry to Enantiomerically Pure Amines and Natural and Unnatural α-Amino Esters. *Org. Lett.* **2009**, *11*, 2928–2931. (g) Li, G.; Antilla, J. C., Highly Enantioselective Hydrogenation of Enamides Catalyzed by Chiral Phosphoric Acids. *Org. Lett.* **2009**, *11*, 1075–1078. (h) Malkov, A. V.; Vranková, K.; Stončius, S.; Kočovský, P., Asymmetric Reduction of Imines with Trichlorosilane, Catalyzed by Sigamide, an Amino Acid-derived Formamide: Scope and Limitations. *J. Org. Chem.* **2009**, *74*, 5839–5849. (i) Bonsignore, M.; Benaglia, M.; Raimondi, L.; Orlandi, M.; Celentano, G., Enantioselective Reduction of Ketoimines Promoted by Easily Available (*S*)-Proline Derivatives. *Beilstein J. Org. Chem.* **2013**, *9*, 633–640. (j) Wen, W.; Zeng, Y.; Peng, L.-Y.; Fu, L.-N.; Guo, Q.-X., Asymmetric Synthesis of α-Amino Ketones by Brønsted Acid Catalysis. *Org. Lett.* **2015**, *17*, 3922–3925.

(17) (a) Rueping, M.; Sugiono, E.; Azap, C.; Theissmann, T.; Bolte, M., Enantioselective Brønsted Acid Catalyzed Transfer Hydrogenation: Organocatalytic Reduction of Imines. *Org. Lett*. **2005**, *7*, 3781–3783. (b) Rueping, M.; Azap, C.; Sugiono, E.; Theissmann, T., Brønsted Acid Catalysis: Organocatalytic Hydrogenation of Imines. *Synlett* **2005**, *15*, 2367–2369. (c) Fleischmann, M.; Drettwan, D.; Sugiono, E.; Rueping, M.; Gschwind, R. M., Brønsted Acid Catalysis: Hydrogen Bonding versus Ion Pairing in Imine Activation. *Angew. Chem. Int. Ed.* **2011**, *50*, 6364–6369. (d) Parmar, D.; Sugiono, E.; Raja, S.; Rueping, M., Complete Field Guide to Asymmetric BINOL-phosphate Derived Brønsted Acid and Metal Catalysis: History and Classification by Mode of Activation; Brønsted Acidity, Hydrogen Bonding, Ion Pairing, and Metal Phosphates. *Chem. Rev.* **2014**, *114*, 9047–9153.

(18) (a) Shibasaki, M.; Kanai, M., Asymmetric Synthesis of Tertiary Alcohols and α-Tertiary Amines via Cu-catalyzed C–C Bond Formation to Ketones and Ketimines. *Chem. Rev.* **2008**, *108*, 2853–2873. (b) Vasu, D.; de Arriba, A.L.F.; Leitch, J. A.; de Gombert, A.; Dixon, D.J., Primary α-Tertiary Amine Synthesis via α-C–H Functionalization. *Chem. Sci.* **2019**, *10*, 3401–3407.

(19) (a) Park, C.; Ryabova, V.; Seregin, I. V.; Sromek, A. W.; Gevorgyan, V., Palladium-catalyzed Arylation and Heteroarylation of Indolizines. *Org. Lett.* **2004**, *6*, 1159–1162. (b) Shu, W.; Nevado, C., Visible-light-mediated Remote Aliphatic C–H Functionalizations Through a 1,5-Hydrogen Transfer Cascade. *Angew. Chem. Int. Ed*. **2017**, *56*, 1881–1884. (c) Chuentragool, P.; Yadagiri, D.; Morita, T.; Sarkar, S.; Parasram, M.; Wang, Y.; Gevorgyan, V., Aliphatic Radical Relay Heck

Reaction at Unactivated C(sp^3)-H Sites of Alcohols. *Angew. Chem. Int. Ed.* **2019**, *58*, 1794–1812.

(20) (a) Zhou, W.-J.; Cao, G.-M.; Shen, G.; Zhu, X.-Y.; Gui, Y.-Y.; Ye, J.-H.; Sun, L.; Liao, L.-L.; Li, J.; Yu, D.-G., Visible-light-driven Palladium-catalyzed Radical Alkylation of C–H Bonds with Unactivated Alkyl Bromides. *Angew. Chem. Int. Ed.* **2017**, *56*, 15683–15687. (b) Sun, L.; Ye, J.-H.; Zhou, W.-J.; Zeng, X.; Yu, D.-G., Oxy-alkylation of Allylamines with Unactivated Alkyl Bromides and CO_2 via Visible-light-Driven Palladium Catalysis. *Org. Lett.* **2018**, *20*, 3049–3052.

(21) (a) Prier, C. K.; Rankic, D. A.; MacMillan, D. W. C., Visible Light Photoredox Catalysis with Transition Metal Complexes: Applications in Organic Synthesis. *Chem. Rev.* **2013**, *113*, 5322–5363. (b) Skubi, K. L.; Blum, T. R.; Yoon, T. P., Dual Catalysis Strategies in Photochemical Synthesis. *Chem. Rev.* **2016**, *116*, 10035–10074. (c) Yan, M.; Lo, J. C.; Edwards, J. T.; Baran, P. S., Radicals: Reactive Intermediates with Translational Potential. *J. Am. Chem. Soc.* **2016**, *138*, 12692–17714. (d) Douglas, J. J.; Sevrin, M. J.; Stephenson, C. R. J., Visible Light Photo Catalysis: Applications and New Disconnections in the Synthesis of Pharmaceutical Agents. *Org. Process Res. Dev.* **2016**, *20*, 1134–1147. (e) Shaw, M. H.; Twilton, J.; MacMillan, D. W. C., Photoredox Catalysis in Organic Chemistry. *J. Org. Chem.* **2016**, *81*, 6898–6926. (f) Romero, N. A.; Nicewicz, D. A., Organic Photoredox Catalysis. *Chem. Rev.* **2016**, *116*, 10075–10166.

(22) (a) Falivene, L.; Kozlov, S. M.; Cavallo, L., Constructing Bridges between Computational Tools in Heterogeneous and Homogeneous Catalysis. *ACS Catal.* **2018**, *8*, 5637–5656. (b) Kancherla, R.; Muralirajan, K.; Maity, B.; Zhu, C.; Krach, P. E.; Cavallo, L.; Rueping, M., Organic Photoredox Catalysis. *Angew. Chem. Int. Ed.* **2019**, *58*, 3412–3454.

(23) (a) Griller, D.; Ingold, K. U., Free-radical Clocks. *Acc. Chem. Res.* **1980**, *13*, 317–323. (b) Noda, D.; Sunada, Y.; Hatakeyama, T.; Nakamura, M.; Nagashima, H., Effect of TMEDA on Iron-catalyzed Coupling Reactions of ArMgX with Alkyl Halides. *J. Am. Chem. Soc.* **2009**, *131*, 6078–6079. (c) Fawcett, A.; Pradeilles, J.; Wang, Y.-H.; Mutsuga, T.; Myers, E. L.; Aggarwal, V. K., Photoinduced Decarboxylative Borylation of Carboxylic Acids. *Science* **2017**, *357*, 283–286.

(24) All (DFT) alculations were performed by Gaussian 09 program. The single-point energies and solvent effects were computed with the M06 functional using the SDD basis set for palladium and the 6-311+G(d,p) basis set for the other atoms. The solvation energies were evaluated by a self-consistent reaction field using the SMD implicit solvent model. Further details are given in the Supporting Information.

(25) (a) García-Melchor, M.; Braga, A. A. C.; Lledos, A.; Ujaque, G.; Maseras, F., Computational Perspective on Pd-catalyzed C-C Cross-coupling Reaction Mechanisms. *Acc. Chem. Res.* **2013**, *46*, 2626–2634. (b) Sperger, T.; Sanhueza, I. A.; Kalvet, I.; Schoenebeck, F., Computational Studies of Synthetically Relevant Homogeneous Organometallic Catalysis Involving Ni, Pd, Ir, and Rh: an Overview of Commonly Employed DFT Methods and Mechanistic Insights. *Chem. Rev.* **2015**, *115*, 9532–9586.

(26) (a) Marcus, R. A., On the Theory of Electron-transfer Reactions. VI. Unified Treatment for Homogeneous and Electrode Reactions. *J. Chem. Phys.* **1965**, *43*, 679–701. (b) Marcus, R. A.; Sutin, N., Electron Transfers in Chemistry and Biology. *Biophys. Acta* **1985**, *811*, 265–322. (c) Silverstein, T. P., Marcus Theory: Thermodynamics can Control the Kinetics of Electron Transfer Reactions. *J. Chem. Educ.* **2012**, *89*, 1159–1167.

TOC

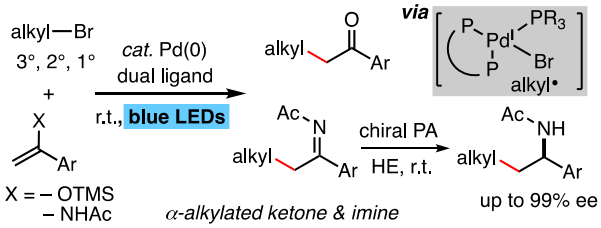
alkyl—Br
3°, 2°, 1°
+
X
Ar
X = – OTMS
– NHAc
cat. Pd(0)
dual ligand
r.t., blue LEDs
alkyl
O
Ar
via
P
Pd
PR3
P
Br
alkyl•
Ac
N
alkyl
Ar
chiral PA
HE, r.t.
Ac
NH
alkyl
Ar
up to 99% ee
α-alkylated ketone & imine